Global Journal of Engineering and Technology Advances

eISSN: 2582-5003

Cross Ref DOI: 10.30574/gjeta

Journal homepage: https://gjeta.com/

(Research Article)

Check for updates

# Application of finite difference method to 2D heat conduction in young hydrating mass concretes structures.

Ugwuanyi Donald Chidiebere *

*Department of Civil Engineering, Enugu State University of Science and Technology, Nigeria.*

Global Journal of Engineering and Technology Advances, 2023, 17(03), 054–060

Publication history: Received on 15 November 2023; revised on 27 December 2023; accepted on 29 December 2023

Article DOI: https://doi.org/10.30574/gjeta.2023.17.3.0248

## Abstract

Finite Difference Method is a numerical approximation scheme usually applied in solving differential equations derived from the knowledge of the behaviour of engineering systems. Due to the unsteady state nature of cement hydration and heat conduction in concretes, Crank Nicholson implicit approach was adopted. Concrete block of size 1.10 m x 1.10 m x 1.10 m, cast with mix ratio 1:3:6, probed thermocouples and digital thermometer were used to verify the numerical computational analysis. The temperature profile depicted a relatively hot core, with peak temperature values occurring at 24 hours of placement. Implicit finite difference method was utilized in determining time dependent temperature profile within mass concretes at early ages. The paper could provide a guide towards proactive decision making in terms of controlling thermal cracks.

**Keywords**: Finite Difference; Implicit; Temperature; Time and Mass Concrete; Cracks.

## 1. Introduction

Cracks due to temperature difference is always envisaged in mass concretes because of the uneven expansion and contraction between the core and the surface. Concretes whose dimension is such that its conduct when exposed to heat could result to cracks unless appropriate preventive procedures are devised are called mass concretes [ 1, 2]. Restraint arises from the unequal thermal expansivity that takes place across the mass concretes. This will induce stresses, whose nature will be tensile at the exterior and compressive at the core. When the exterior stresses which is tensile in kind, an import of the wide-ranging forces that transpire within, becomes greater than the strength of the concretes, hairline cracks will evolve and may magnify at the exterior. Temperature is monitored in mass concretes in order to control cracking and aspects linked to longevity. Cracks lead to disruptions in concretes due to chance of corrosion that may be caused by chloride ions percolating into reinforcement steel via the cracks [ 3, 4]. Thermal cracks depend on the degree of uneven temperature across the mass concretes and the vicinity temperature conditions.

[5] developed finite element model for distortion and cracking in newly batched concrete. [6] studied thermal crack of young hydrating mass concretes using extended finite element method (XFEM) through thermal fields and creep. [7] evolved a material model to ascertain the stresses and the width of crack engendered by hydration heat in mass concretes. [8] used finite element-based simulation to model temperature variance in thick rafts at early ages. Core objective of the study was to apply Crank-Nicholson implicit finite difference method to 2D heat conduction in early age hydrating mass concretes.

* Corresponding author: Ugwuanyi Donald Chidiebere.

## 2. Methodology

Hydrating concrete is a self-heat generating system and it was assumed that the material constituents of the concrete is isotropic, therefore the thermal conductivity will remain constant in all directions. A suitable governing equation, which is a 2D unsteady state heat conduction equation in Equation (1) was adopted thus;

$$K\left(\frac{\partial^2 T}{\partial x^2}+\frac{\partial^2 T}{\partial y^2}\right)+\ q\ =\rho Cp\frac{\partial T}{\partial t} \quad (1)$$

$\rho$ is density (kg/m$^3$), $C_P$ is specific heat capacity (J/kg.$^0$C), $q$ is heat intensity (KJ/m$^3$.h), K is thermal conductivity (KJ/m.h$^0$C), $T$ is temperature ($^0$C) and t is time (hrs).

The numerical solution process used the Crank-Nicholson implicit finite difference method, an approximation scheme that is second order accurate both in time and space. This makes the analytical procedure unconditionally stable so that you can take any time steps.

$$T(0,y,t) = T(a,y,t) = T_a \quad (2)$$

$$T(x,0,t) = T(x,b,t) = T_a \quad (3)$$

$T_a$ is ambient temperature.

Initial conditions:

$$T\ (x,y,0) = T_0 \quad (4)$$

$T_0$ is initial placement temperature.

$$\rho Cp\frac{\left(T_{i1j}^{k+1}-T_{i1j}^{k}\right)}{\Delta t}=\ K\frac{\left(T_{i+1,j}-2T_{i1j}+T_{i-1,j}\right)}{(\Delta x)^2}\ +K\frac{\left(T_{i,j+1}-2T_{i1j}+T_{i,j-1}\right)}{(\Delta y)^2}+\ \ q_{i,j}^{k} \quad (5)$$

$$T_{i1j}^{k+1}-T_{i1j}^{k}=\frac{K\Delta t}{\rho Cp\ (\Delta x)^2}\left(T_{i+1,j}-2T_{i1j}+\ T_{i-1,j}\right)\ +\frac{K\Delta t}{\rho Cp\ (\Delta y)^2}\left(T_{i,j+1}-2T_{i1j}+\ T_{i,j-1}\right)+\frac{\Delta t}{\rho Cp}q_{i,j}^{k} \quad (6)$$

$$T_P^{k+1}-T_p^{k}=\frac{K\Delta t}{\rho Cp\ (\Delta x)^2}\left[T_E-2T_P+T_W\right]+\frac{K\Delta t}{\rho Cp\ (\Delta y)^2}\left[T_N-2T_P+T_S\right]+\frac{\Delta t}{\rho Cp}q_P^{k} \quad (7)$$

$$T_n = f\,T_n^{k+1}+(1-f)T_n^{k} \quad (8)$$

$$T_P^{k+1}-T_p^{k}=\frac{K\Delta t}{\rho Cp\ (\Delta x)^2}\left[f\,T_E^{k+1}+(1-f)T_E^{k}+f\,T_W^{K+1}+(1-f)T_W^{K}-2T_P+T_W-2f\,T_P^{k+1}-2(1-f)T_S^{K}\right]+\frac{K\Delta t}{\rho Cp\ (\Delta y)^2}\left[f\,T_N^{k+1}+(1-f)T_N^{k}+f\,T_S^{K+1}+(1-f)T_S^{K}-2f\,T_P^{K}\right]+\frac{\Delta t}{\rho Cp}q_P^{K} \quad (9)$$

Taking f as $^1/_2$,

$$T_P^{k+1}-T_p^{k}=\frac{K\Delta t}{\rho Cp\ (\Delta x)^2}\left[\frac{1}{2}\ T_E^{k+1}+\frac{1}{2}T_E^{k}+\frac{1}{2}T_W^{K+1}+\frac{1}{2}T_W^{K}-T_P^{k+1}-T_P^{K}\right]\ \frac{K\Delta t}{\rho Cp\ (\Delta y)^2}\left[\frac{1}{2}\ T_N^{k+1}+\frac{1}{2}T_N^{k}+\frac{1}{2}T_S^{K+1}+\frac{1}{2}T_S^{K}-T_P^{k+1}-T_P^{K}\right]+\frac{\Delta t}{\rho Cp}q_P^{K} \quad (10)$$

$$T_P^{k+1}\left[1+\frac{K\Delta t}{\rho Cp(\Delta x)^2}+\frac{K\Delta t}{\rho Cp(\Delta y)^2}\right]-\frac{K\Delta t}{2\rho Cp(\Delta x)^2}\left[T_E^{k+1}+T_W^{k+1}\right]-\frac{K\Delta t}{\rho Cp(\Delta y)^2}\left[T_N^{k+1}+T_S^{k+1}\right]$$
$$=T_P^{k}\left[1-\frac{K\Delta t}{\rho Cp(\Delta x)^2}-\frac{K\Delta t}{\rho Cp(\Delta y)^2}\right]+\frac{K\Delta t}{2\rho Cp(\Delta x)^2}\left[T_E^{k}+T_W^{k}\right]+\frac{K\Delta t}{2\rho Cp(\Delta xy)^2}\left[T_N^{k}+T_S^{k}\right]$$
$$+\frac{K\Delta t}{\rho Cp}q_P^K \quad (11)$$

A cubic mass concrete of size 1.10m x 1.10m x 1.10m and mix ratio 1 : 3 : 6 was used to verify the numerical solution. Thermocouples and digital thermometer were used to measure temperatures with time. Temperature values were determined at time intervals of 2, 12, 18, 24, 48, 72, 96, 120 and 144 hours. MATLAB program was developed to evaluate Equation (11) as part of the solution process. The input variables are the initial and ambient temperatures, parameters such as thermal conductivity, density and specific heat capacity, the size of the mass concrete and time steps. The output variables are spreadsheet file containing the nodal temperatures.

## 3. Results

Temperature readings were taken from thermocouples located at the core, top, bottom and side of the mass concrete, which was further compared with that of the analytical procedure. The temperature time data from the experimental procedure in Figure 1 showed uniform initial temperature which rose to its peak at 24 hours of concrete placement and subsequently declined to the prevailing ambient temperature. The core of the mass concrete generally had higher temperatures than the rest of the thermocouple locations with the highest temperature of $41^0$C occurring at 24 hours. The thermocouple located at the bottom of the mass concrete generally had lower temperature values, this is attributable to the fact that it is affected by the temperature of the ground on which the mass concrete was founded. On the other hand, the temperature time data from the analytical procedure in Figure 2 showed core temperatures that are well above the other locations which exhibited fairly uniform temperature values at all times. The highest core temperature of $56.59^0$C occured at 24 hours.

Data from the experimental and analytical procedures were further compared at each of the thermocouple locations as shown in Figures 3 to 6, which indicates that the analytical temperature values made an acceptable prediction of the experimental inferences. This was corroborated by the coefficient of determination ($R^2$) that had values of 0.9015, 0.7137, 0.8421 and 0.8757 as shown in Figures 7 to 10 at the top, core, bottom and side respectively.

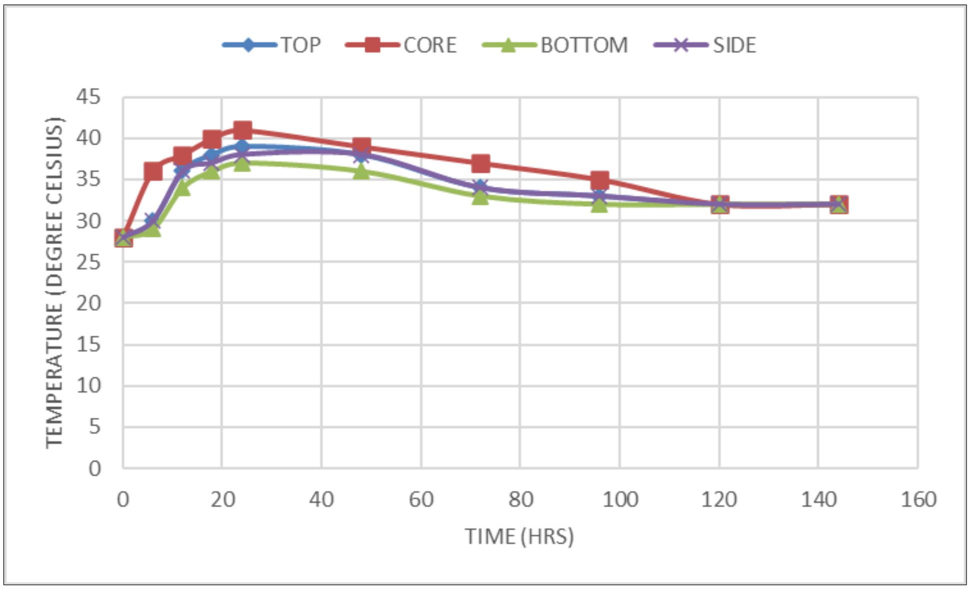


**Figure 1** Temperature time graphs of the experimental data.

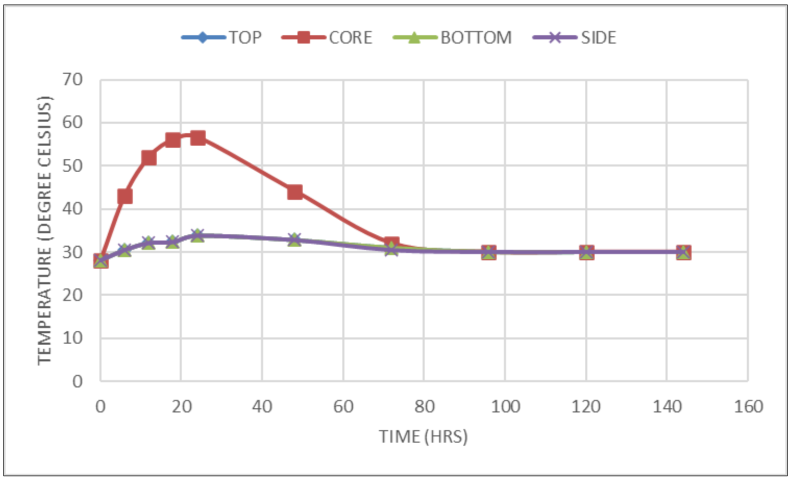


**Figure 2** Temperature time graphs of the analytical data.

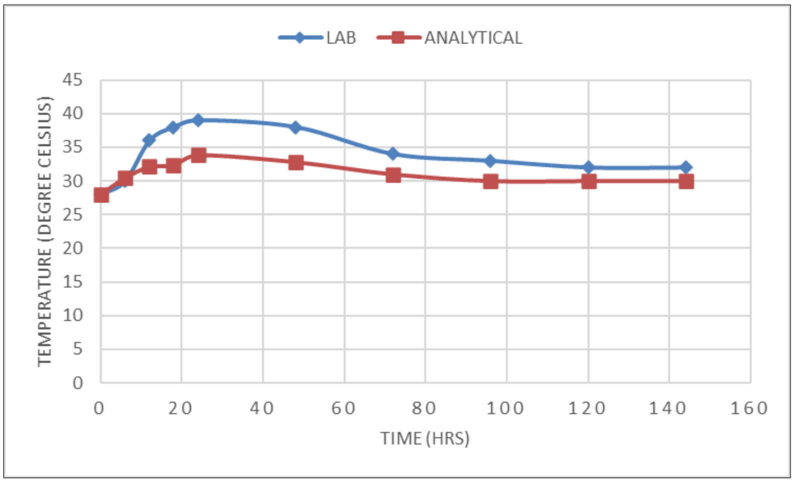


**Figure 3** Temperature-time graphs of experimental and analytical data (Top)

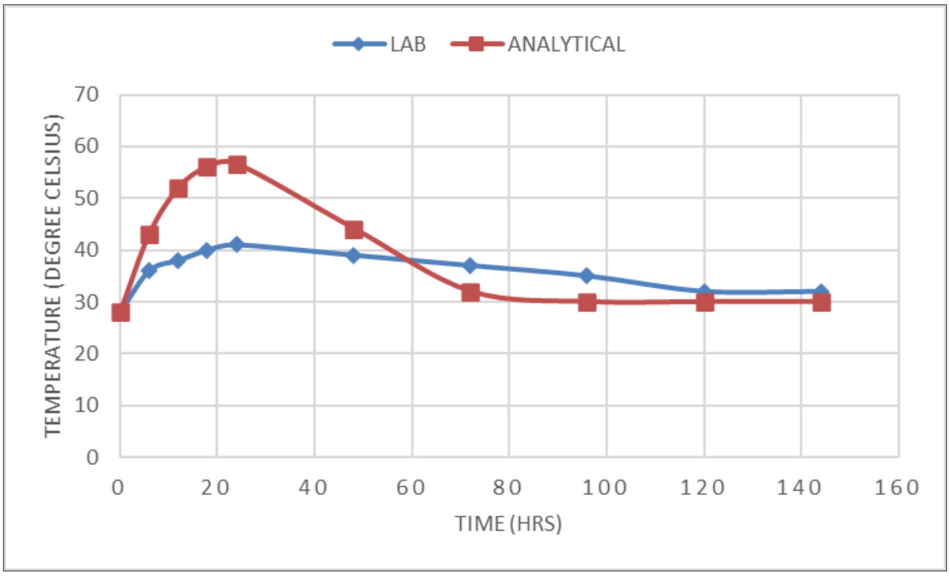


**Figure 4** Temperature-time graphs of experimental and analytical data (Core)

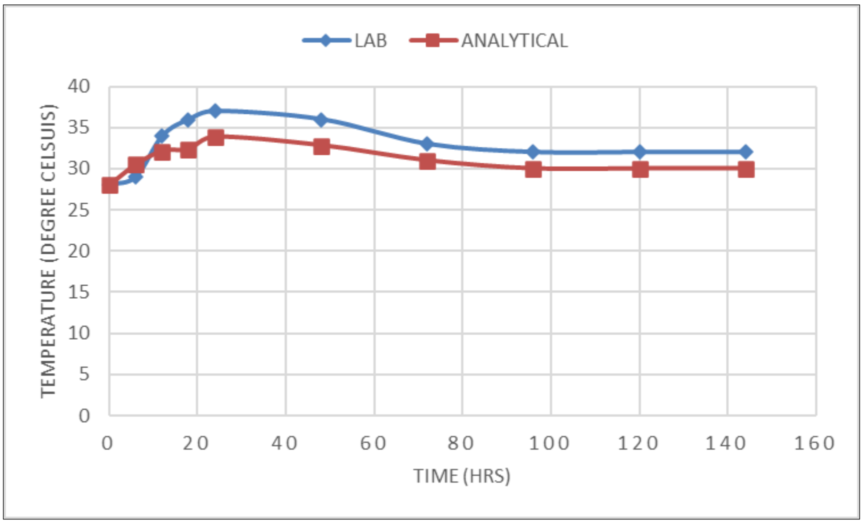


**Figure 5** Temperature-time graphs of experimental and analytical data (Bottom)

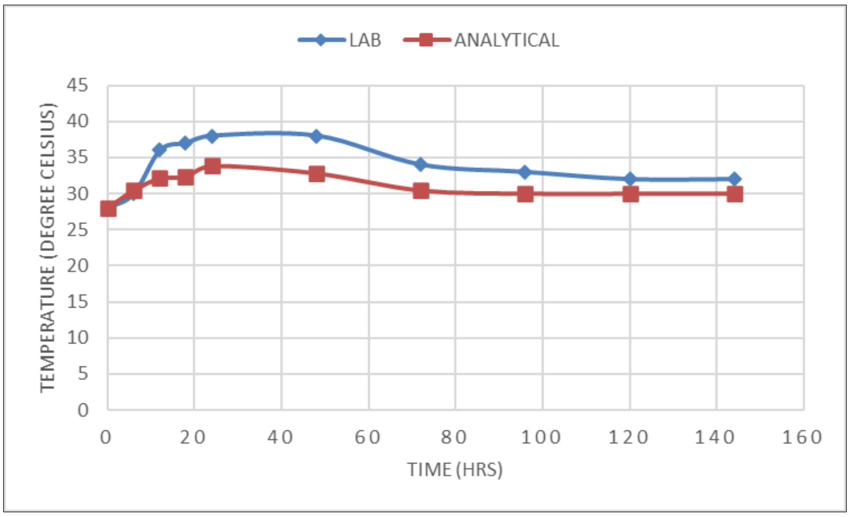


**Figure 6** Temperature-time graphs of experimental and analytical data (Side)

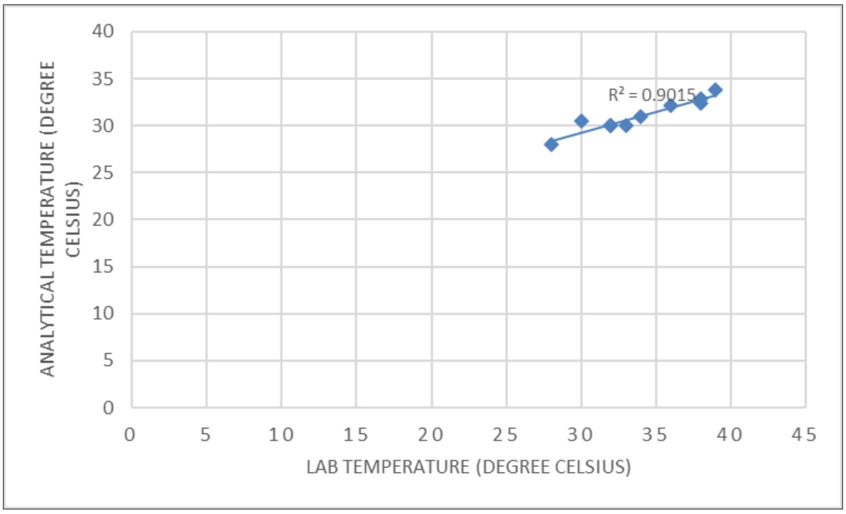


**Figure 7** Coefficient of determination of experimental and analytical temperatures (Top)

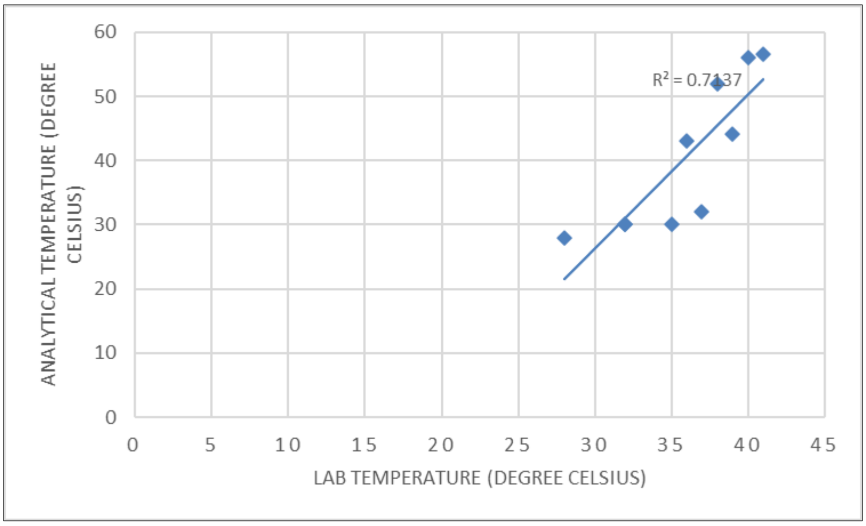


**Figure 8** Coefficient of determination of experimental and analytical temperatures (Core)

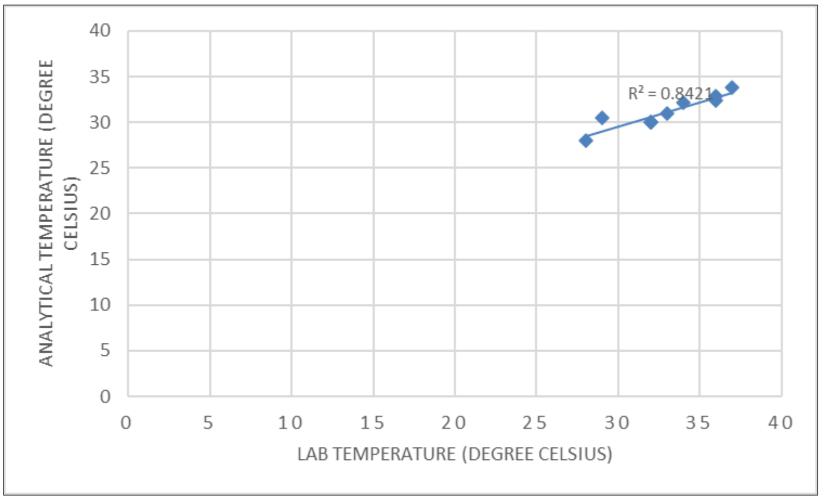


**Figure 9** Coefficient of determination of experimental and analytical temperatures (Bottom)

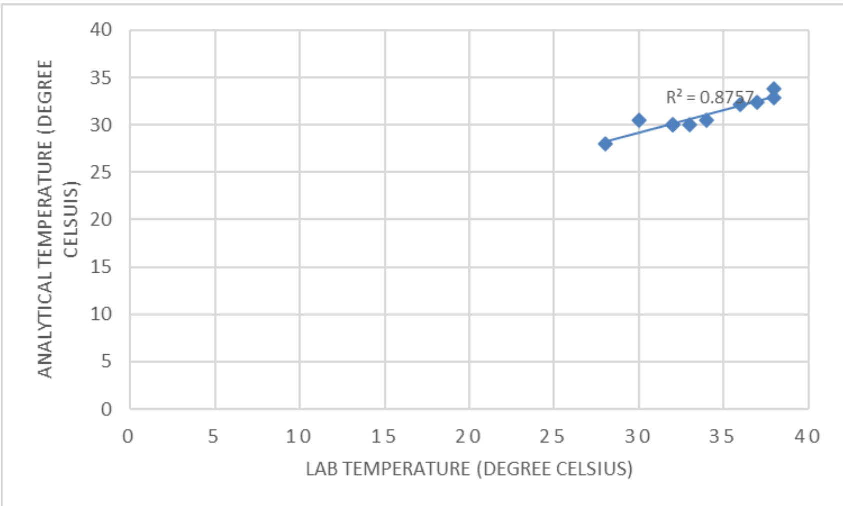


**Figure 10** Coefficient of determination of experimental and analytical temperatures (Side)

## 4. Conclusion

Implicit finite difference was successfully applied in the analysis of 2D heat conduction in early age hydrating mass concrete using the Crank-Nicholson implicit approach. Experimental procedures were conducted in order to verify the efficacy of the time dependent temperature data obtained from the analytical processes. Generally, there was substantial temperature gradient between the center (core) and the surface which if not properly controlled could lead to thermal cracks. The peak temperatures occurred within 24 hours of concrete placement. The analytical processes as contained in this paper could help in taking proactive measures to prevent potential cracks if they are strictly adhered to.

## Reference

[1] Neville, A. M (2011): Properties of Concrete, 5th Edition, Longman Scientific and Technical Publishing, London, pp. 1279-1292.

[2] ACI Committee 207, (2005): Guide to Mass Concrete, ACI Committee 207, American Concrete Institute Farmington Hill, Mich.

[3] Worapong, S., Nakamura, H., Kunieda, M., & Ishikawa, Y. (2007): Analysis of Crack Propagation Due to Thermal Stress in Concrete Considering Slodified Constitutive Model, Journal of Advanced Concrete Technology, Vol. 5, No. 1, pp. 99-112.

[4] Srisoros, W., Nakamura, H., Kunieda, M., & Ishikawa, Y. (2007): Analysis of Crack Propagation Due to Thermal Stress in Concrete Considering Solidified Constitutive Model, Journal of Advanced Concrete Technology, Vol. 5, No. 1, pp. 99-112.

[5] Borst, R., & Boogaard, A. H. (1994): Finite Element Modeling of Deformation and Cracking in Early-Age Concrete, Journal of Engineering Mechanics, Vol. 120. no. 12. pp. 2519-2534.

[6] Liu, G., Hu, Y., Li, Q., & Zuo, Z. (2013): XFEM for Thermal Cracks of Massive Concrete, Mathematical Problems in Engineering, Vol. 2013, http://dx.doi.org/10.1155/2013/343842.

[7] Bazant, Z. P., Kim, J. K., & Jeon, S. E. (2003): Cohesive Fracturing and Stress Caused by Hydration Heat in Massive Concrete Wall, Journal of Engineering Mechanics, DOI: 10.1061/(ASCE) 0733-9399 (2003) 129: 1 (21).

[8] Kuriakose, B., B. N. Rao., Dodagoudar, G. R., Modeling of early age concrete temperature distribution in thick rafts, 5th International Congress on Computational Mechanics and Simulation, (2014) 10 -13.